Journal of Engineering
journal homepage: www.joe.uobaghdad.edu.iq
Number 8 Volume 25 August 2019

Chemical, Petroleum and Environmental Engineering

Comparison Study of Adsorption of Lead and Methylene Blue on Zeolite, Activated Carbon and Their Composite Materials

Rafie Rushdy Mohammed
Assistant Professor
Northern Technical University, Iraq
rafie.rushdy@ntu.edu.iq, Rafie59.che@gmail.com

ABSTRACT

In this study, composite materials consisting of Activated Carbon (AC) and Zeolite were prepared for application in the removal of methylene blue and lead from an aqueous solution. The optimum synthesis method involves the use of metakaolinization and zeolitization, in the presence of activated carbon from kaolin, to form Zeolite. First, Kaolin was thermally activated into amorphous kaolin (metakaolinization); then the resultant metakaolin was attacked by alkaline, transforming it into crystalline zeolite (zeolitization). Using nitrogen adsorption and SEM techniques, the examination and characterization of composite materials confirmed the presence of a homogenous distribution of Zeolite throughout the activated carbon. It has also shown the carbonization process did not destroy the crystalline structure of the zeolite, which was revealed to be intact. Experiments in batch mode were conducted (using three differently-prepared composites, zeolite and activated carbon), to investigate the removal of methylene blue and lead from the aqueous solution of the sorbents. Key experimental parameters (initial concentration, pH, contact time and adsorbent dosage) from the obtained results were measured and analysed. Freundlich and Langmuir models were used to describe the adsorption isotherms, and the observed adsorption kinetic adhered to pseudo-second order.

Keywords: Adsorption, isotherm, kinetics, zeolite; activated carbon

دراسة مقارنة لامتزاز الرصاص والميثيلين الأزرق على الزيوليت، الكربون المنشط والمواد المركبة منهما

رافع رشدي محمد
استاذ مساعد

الخلاصة

تم في هذه الدراسة تحضير مواد مركبة تتألف من الفحم المنشط والزيةلايت لإستخدامها في ازالة الرصاص وصبغة المثيلين الزرقاء من محاليلها المائية. طريقة التحضير المثلى تأخذ بنظر الاعتبار تكوين الزيولايت بوجود الفحم المنشط من الكاؤلين خلال عملية تكوين الميتاكاؤلين والزيولايت. ينشط الكاؤلين حراريا ليتحول الى كاؤلين غير متبلور ومن ثم يعامل مع قاعدة لتحويله الى زيولايت متبلور. تم تحديد مواصفات المواد المركبة بواسطة امتزاز النايتروجين وناظور

---

*Corresponding author

Peer review under the responsibility of University of Baghdad.
https://doi.org/10.31026/j.eng.2019.08.09

Article received: 9/10/2016
Article accepted: 20/2/2017

المسح الالكتروني والتي اوضحت توزيع الزيولايت بشكل متجانس خلال الفحم المنشط واكدت التركيب المتبلور للزيولابيت، أي أن هيكلية الزيولايت لم يتم تدميرها بواسطة عملية الكربنة. تم اختبار قابلية ازالة صبغة المثيلين الزرقاء والرصاص من محاليلها المائية بطريقة الدفعات باستخدام الكاربون المنشط والزيولايت وثلاث مواد مركبة بطرق مختلفة منهما. التجارب ايضا اختبرت تأثير العديد من العوامل المؤثرة ومنها الدالة الحامضية، تركيز المادة المازة، التركيز الابتدائي وزمن التلامس. منحنيات الامتزاز تم توصيفها بنجاح بواسطة نماذج لانكماير وفرندلخ وحركية التفاعل تنطبق عليها نظرية الدرجة الثانية الزائفة.

الكلمات الرئيسية: الامتزاز، منحنيات الامتزاز، حركية التفاعل، الزيولايت و الكاربون المنشط.

1. INTRODUCTION

One of the most serious of environmental issues today is the chemical contamination of waters by a plethora of derivatives - notably dyes, aromatic molecules and heavy metals – that are potential toxic to humans. For instance, in its solid form Lead is a material that is widely used across a range of applications, including solder, ammunition, cable covering, bearings, waste pipelines, radiation shielding and storage batteries. As a poisonous heavy metal, it can adversely affect human metabolic processes and damage cardiovascular functions, particularly in children, **Eisazadeh, 2013**. Consequently, the concentration of Lead in drinking water is generally limited to a maximum of 0.05 mg/L by the drinking water standard (USPHS). A range of industrial sectors and applications, including plastic, fabrics, food colouring, papermaking, and cosmetics produce large quantities of wastewaters, which represent a major source of coloured effluents. A major concern over the past decade has thus been the increasing water contamination caused by the direct discharge of such toxic dyes into water bodies.

The most widely used material for dying wool, silk and cotton, Methylene blue (MB) is also known for a number of hazardous effects on humans and animals. For instance, when ingested it can result in mental confusion, nausea, methemoglobinemia, vomiting, profuse sweating and burning sensations, **Ghosh, and Bhattacharyya, 2002**. MB can also cause permanent damage to the eyes on contact, and severe respiratory difficulties when inhaled. In this context, it is extremely important, from both environmental and health perspectives, for the presence of MB in waste effluents to be minimised and, ultimately, eliminated. A range of techniques, including precipitation, electro-deposition, flotation, extraction, coagulation and ion exchange, **Standeker, et al., 2007**, which involve both physical and chemical processes, can be deployed to address the issue of heavy metals contamination of water solutions. One of such solutions is adsorption by the use of solvents. As a notable method in the context of equilibrium separation and analysis, adsorption through the use of sorbents is a widely-adopted technique in this regard. This is not only because it is an efficient and economic method for decontaminating aqueous solutions, but also because it is highly effective in producing first-rate effluents.

The most commonly used adsorbents in this regard include Zeolites, **Kamble, et al., 2008, and Ruchi, et al., 2016**, some industrial by-products (low-cost adsorbents), **Garg, et al., 2003, Haochun, et al., 2014, and Akl, et al., 2016**, ceramic materials, **Dabrowski, et al., 2005**, resin, **Ming, et al., 2010**, agricultural waste, **Ebrahimian, et al., 2015, Torrellas, et al., 2016, and Nnaji, et al., 2017**, activated carbons, **Rhoda, 2016, and Legrouri, et al., 2017**, clays, **Tholiso, et al., 2017**, and bio-sorbents, **Shisuo, et al., 2017**.
Zeolites and Activated Carbon represent two of the most commonly-adopted adsorbents in use today. Due to its virtually microporous, polymodal structure; its high-absorption capabilities; as well as the large and variable chemical composition of its surface area,

Activated Carbon offers the greatest degree of versatility among adsorbents, **Giraldo and Piraján, 2008**. Composed of a network of tetrahedral molecules connected via shared O_2 atoms, Zeolites are naturally-occurring, microporous, aluminosilicate materials which exhibit (due to their crystalline structure) great acidity characteristics which can be highly valuable in the context of water treatment, especially for catalytic, purification and separation applications. Due to their high-cation exchange capacity and large surface area, Zeolites present an exchange complex for removing different ions, **Babel and Kurniawan, 2003**. They are also more cost-effective than activated carbon for the removal of heavy metals from contaminated waters, **Sublet, et al., 2003**. The use of zeolites has also been observed to produce highly-efficient rates of lead ion removal,**Ouki, and Kavannagh, 1999, Petruzzelli, et al., 1999, Chen, 2001, and Panayotova and Velikov, 2002**. Meanwhile, after screening twelve (12) sorbents, including acid-washed reagent-grade zeolite and activated carbon, Olin and Bricka, **Olin and Bricka, 1998** established that zeolites produced the highest Lead ion removal rate.

Several investigations have been undertaken to examine the Adsorption features of MB on a range of adsorbents. For instance, a study by Senthil Kumar et al., established that fly ash was an adequate adsorbent for MB-removal, **Kumar, et al., 2005**, while another study found that kaolinite clay could be effective for eliminating MB at low concentrations, **Ghosh and Bhattacharyya, 2002**.

Further studies have examined the adsorption of MB by a variety of other materials, including stainless steel surface, **Imamura, et al., 2002**, wood sawdust, **Shukla, et al., 2002**, clay, **Gurses, et al., 2004**, perlite, **Doğan, et al., 2004**, jute fibre, **Chakrabarti and Dutta, 2005**, rice husk, **Vadivelan and Kumar, 2005**, glass fibre carbon, K**umaar, et al., 2005**, wheat shells, **Bulut and Aydin, 2006**, tea waste, **Uddin, et al., 2009**, low-cost bio-sorbents, **Rafatullah, et al., 2010**, rejected tea, **Nasuha, et al., 2010**, peanut shells, **Krowiak, et al., 2011**, tea waste/$CuFe_2O_4$,**Hashemian, et al., 2013** and dead leaves of plane trees, **Gong, et al., 2013**.

In light of this, the present work introduces a novel composite material which offers many of the properties that are advantageous for MB removal - including many of the advantages offered by both zeolites and activated carbon - in a single composite material. In structural terms, this composite material inter crosses two self-assisting but independent networks: a zeolite network featuring a sharpened-pore size distribution, on the one hand, and a carbon network featuring carbonaceous high-activity micro-domains, on the other. In order to overcome the intrinsic disadvantages of using adsorbents that are solely composed of zeolites or activated carbon, respectively, a number of studies in the past few years have examined the environmental applications of Zeolite-Activated Carbon composites, notably their gas separation and waste-water decontamination properties, **Foo and Hameed, 2011**.

In this context, the aim of the present study is to investigate the MB-adsorption properties of Zeolite X-Activated Carbon composites that have been prepared using a range of techniques. This was aimed at producing a new composite which exhibits the benefits offered by both zeolites and activated carbon-based adsorbents. In particular, the investigation involved observing the respective impact of key parameters, such as the solution pH, adsorbent dosage and contact time of each composite.

2. MATERIALS AND METHODS

2.1 Materials

For the purposes of the present study, two commercially-available adsorbents – Zeolite and Activated Carbon (AC) - were used. Naturally-occurring zeolite, which was free of any chemical modifications, was sieved so as to obtain particles of the desired [1.18 mm – 2.00 mm] size range. Distilled water was used to repeatedly rinse both adsorbents, so as to remove any traces of impurities (such as dust). The adsorbents were then oven-heated for a period of 24 hours at a temperature of 105ºC, and subsequently dried for two hours in a desiccator.

The principal materials for the experiments undertaken in the present work, including Kaolin, Bentonite, CarboxyMethylCelullose (CMC), Methylene Blue (MB), lead Nitrate, sodium hydroxide and hydrochloric acid, as well as the Zeolite and AC adsorbents, were all supplied by Sigma-Aldrich, UK.

2.1.1 Preparation of MB stock solution

In order to prepare the MB stock solution (1 g/L), the appropriate quantity of cationic dye (CI=52015; chemical formula=$C_{16}H_{18}N_3SCl$; MW=319.86; nature = basic blue and λmax = 660 nm) is measured out and dissolved in double-distilled water. Successive dilutions of the experimental solution are performed until the required concentration is reached. The experiments were conducted at initial pH values ranging from 2 to 10, which were then adjusted through the addition of dilute hydrochloric acid and sodium hydroxide solutions.

The samples' absorbencies were measured using a UV-vis spectrophotometer (Specord 200) operating at a wavelength of 670 nm (this is the wavelength at which MB absorbency is at its maximum). Linear regression equations are subsequently used to measure the samples' respective concentrations. This is performed through plotting the calibration curve for the dye across the relevant range of concentrations.

2.1.2 Preparation of Lead Nitrate Solution

The 1000 mg/l lead nitrate stock solution was obtained by dissolving 1.3 g of lead nitrate into 1L of deionized water (added gradually). A mixing bar was then dropped into the volumetric flask, and the resultant blend mixed until the complete dissolution of the lead. By using the appropriate degree of dilution, a number of samples of the stock solution were produced, each at the required concentration. Until usage, the solution is stirred at room temperature while an aluminium-foil protects the flask from excessive light exposure.

The concentration of lead in the liquid (in ppm) is measured at the end of the reaction period for each reaction flask. This is performed using an appropriately-calibrated atomic absorption spectrophotometer (PERKIN ELMER, A 800, slit = 0.5, wavelength = 228.8 nm, one flame of the air–C_2H_2 type).

2.1.3 Composite Adsorbent Preparation

The set of procedures used in the production of the novel Zeolite-AC composite-based adsorbent discussed in this work is **Mostafa, et al., 2011, Shams, and Mirmohammadi, 2007, and Tepamat, 2014**:

Procedure 1

1- The below-listed set of ingredients were gently mixed using a spatula until a thick slurry was produced:
    a. Zeolite (69 g)
    b. Activated Carbon (69 g)
    c. Kaolin (60 g)
    d. Distilled water (50ml)
2- In order to form a paste, excess water was removed from the slurry.
3- Carboxymethylcelullose (1.38 g) that had been dissolved in distilled water was mixed into the paste. The paste's composition was then evened-out using the spatula.
4- The paste was left to dry partially. Once the water content reached 45%, the paste was pushed through a simple extruder.
5- The resultant spaghetti-like noodles were placed into a pan. They are then left to partially-dry at room temperature for 24 hours.
6- Once dry, the noodles were crushed by being pushed through a standard ASTM sieve, which levels particle size distribution across all samples (i.e. between 20 and 40 standard US mesh).
7- The obtained Na monolith zeolite-AC composite is then calcined in nitrogen atmosphere for three hours using an electrical heater set at 600ºC, which converts the sample's kaolin content into metakaolin. (CMC is burned during this process).

Procedure 2

1- The below-listed set of ingredients were mixed and heated for one hour, starting at room temperature and rising at a heating rate of 5ºC min^{-1} to 600ºC.
    a- Fly ash (47.5 g, collected from a workshop boiler)
    b- Zeolite (32.5 g)
    c- Bentonite (20 g)
    Once the mixture was cooled back down to room temperature, activated carbon (80 g) was added to it and the mix was homogenized.
2- Carboxymethyl cellulose (1.8 g) is dissolved in deionized water (51 ml). The resulting mixture is added to the previous mix and the resulting paste is left for 48 h in order to achieve homogenous levels of moisture.
3- Prior to the forming process, a laboratory pug mill is used to de-air the paste. The paste is then shaped into small green tubes by pushing in through a simple extruder.
4- In order to remove the desired level of absorbed water, the resultant spaghetti-like noodles are dried at 100ºC.
5- Once dried, the noodles are crushed (by being passed through a standard ASTM sieve) so as to ensure the particle size distribution is between 20 and 40 standard US mesh across all samples.
6- Once dried, the test specimens were calcined in Nitrogen atmosphere for 2 hours using a laboratory electrical furnace. The process starts at room temperature before rising at a rate of 5ºC/min until it reaches 500ºC.

Procedure 3

1- Kaolin (222 g) was converted into metakaolin through a calcination process lasting 8 hours at a 800°C temperature.
2- The resulting metakaolin and (111g) of activated carbon was reacted with 3.0M aqueous NaOH solution (the latter obtained by dissolving 132.2 g of NaOH in 1110 ml of distilled water) using covered Teflon beakers (2000 ml capacity). Once the reaction vessel is placed in a water-filled beaker, the combination was put in a heater equipped with both a magnetic stirrer and a thermostat. The reaction vessel was then heated for three hours, ensuring the temperature was maintained between 70 and 80ºC. In light of the slow and time consuming rate of dissolution of metakaolin in sodium hydroxide, the reaction vessel is gently agitated at 350 rpm throughout the heating process so as to help speed the reaction.
3- Once an amorphous aluminosilicate gel is formed, the agitation and heating process is brought to an end. The reaction vessel is then kept unperturbed at room temperature for nucleation, for a period of 72 hours approximately.
4- In order to complete the crystallization process, the reaction vessel is once again placed in the water bath. It is subsequently heated for 4 hours at a temperature of 90ºC while being stirred gently at 350 rpm using a magnetic stirrer.
5- Once the precipitation of the AC-Na-zeolite composite crystals at the bottom of the reaction vessel is complete, simple paper filtration is used to separate the obtained precipitates from the liquid phase. Before the precipitates are collected from the filter paper, it is washed thoroughly until it achieves a pH value of under 11 ($pH < 11$).
6- In the final step, the resulting composite material is dried for ten hours at a temperature of 150ºC, and the particle size distribution is adjusted by passing the samples through a 20 – 40 ASTM standard mesh.

2.2 Sorption Experiments

These tests were performed using Erlenmeyer flasks (250 mL) containing varying quantities (0.5, 1, 1.5, 2 and 2.5 g/l) of adsorbent, and the desired concentrations of Methylene Blue (100 mL) or Pb solution. A horizontal shaker is used to agitate the flasks, allowing for temperature and agitation control. At specific, predetermined intervals (10 – 240 min), the samples were withdrawn from the shaker and separated (using centrifugation at 4500 rpm for 10 min) from the adsorbent. The supernatant was then analysed for both Pb and colour. As indicated in the literature, **Kumar, et al., 2005**, an AAS (Model Shimadzu A660) with a reading of up to ±0.01 mg/L is used for metal identification and analysis. The instrument was calibrated based on a 10-point [0.1- 10 mg/L] standard curve, which was derived from standard reference solutions for Pb or MB. In order to verify the validity of the calibration, a quality control solution was run during the analysis process.

For colour determination (in Platinum Cobalt unit), a spectrophotometer (Model Hach DR2000) for colour was used. In order to obtain consistent reliable averages, the experiments were performed in triplicates. The removal percentage for heavy metals varied in line with the differences in concentrations of heavy metals and their colour before and after experiment. In order to account for any heavy metals and colour that may have leached from each adsorbent, a set of blank tests were performed separately, using all-adsorbent and distilled water (i.e. without metals and colour).

The quantity of MB or Pb adsorbed at any time was calculated according to the following formula:

$$q_t = \frac{(C_o - C_t)V}{W} \qquad (1)$$

whereby:

C_o (mg/L) refers to the initial concentration level.

C_t (mg/L) refers to the solution concentration of MB or Pb, post-reaction, for a period of time t.

V(L) is the solution volume

W(g) is the weight of adsorbent in a single container.

Batch pH studies were also performed by shaking 100 ml of dye or metal solution (containing approximately 250 mg/l of MB or Pb with 0.2 g of adsorbent) for a period of four hours. This was conducted for a range of initial pH values rising from 2 to 12. Meanwhile, 0.1 N NaOH and 0.1 N HCl solutions were used to adjust the stock solution’s pH level. The reaction mixture’s final pH was subsequently recorded. Throughout the process, a pH meter (HANNA-8417) was used for the adjustment of pH. The experiments were repeated, and the obtained averages were adopted for use in the data analysis. An optimal pH value was also established for use in further studies. Once this optimum pH was determined, isotherm tests were performed at room temperature (298 K) by changing MB and Pb concentration in water. These tests used a range of representative concentrations (25, 50, 100,…, 1000 mg/l). Moreover, 0.2 g of adsorbent was mixed with 100 ml of stock solution for 5 hours, amply sufficient to allow the solution to reach equilibrium at a constant agitation speed of 150 rpm. Once determined, the optimal pH level was subsequently set as the initial pH of solutions used in the experiment. For its part, the final concentration was determined at the end of the study, after the filtering of the samples. All experiments were conducted in duplicate in order to test the reproducibility of the results, and the latter was found to be within the +2% range.

2.3 Characterization

2.3.1 Determination of Surface Area

The characterization of the adsorbent samples was performed by measuring their surface area. To this end, Nitrogen gas was utilised for the adsorption, and surface areas were calculated using Micromeritics ASAP-2000 and based on the BET N_2 method.

2.3.2 SEM studies

In order to examine the pore structure of the adsorbent’s surface, SEM studies were conducted using an Electron Probe Micro Analyzer (Model: Jeol-JXA 840 A, Japan). An essential requirement in this regard is that adsorbent samples should completely moisture-free. Using a conductive adhesive, the pulverised sample was hooked onto a substrate. An essential requirement for conducting SEM testing on a non-conducting specimen is to coat the latter with a skinny film of conducting material. In the present study, this was performed with a gold metal, and used vacuum evaporation to achieve uniform specimen-thickness during the tests.

3. RESULTS AND DISCUSSION

3.1 Adsorbent Characterization

SEM-obtained images of the new zeolite-AC composites (COM1, COM2, and COM3), produced from procedures 1, 2 and 3 respectively, are provided in **Fig.1**. The images in **Fig.1**(a and b) confirm that the zeolite particles were deposited with a modest degree of aggregation on the surface of the activated carbon. This indicates that the zeolite and AC powder cannot homogeneously blend with the binder substances.

Meanwhile, the obtained images of COM3 (provided in **Fig.1**(c)) show this sample features the best mixing of the samples under examination. In this case, as the AC powder agglomerated, it formed numerous bulk regions within the sample, thus enhancing the morphology of the prepared samples. This seems to confirm the excellent adsorption qualities of zeolite and AC, both of which promote adsorption binder substances during the blending process, consequently producing a superior morphology. This morphological property emphasises the large specific area due to the porous structure which is conductive to high uptake of sorbate. As an end result, the respective surface areas for COM1, COM 2, and COM 3 were determined to be 654 m^2/g, 812 m^2/g, and 1024 m^2/g respectively. These increases might have been generated by the acceleration of the homogeneous mixing station.

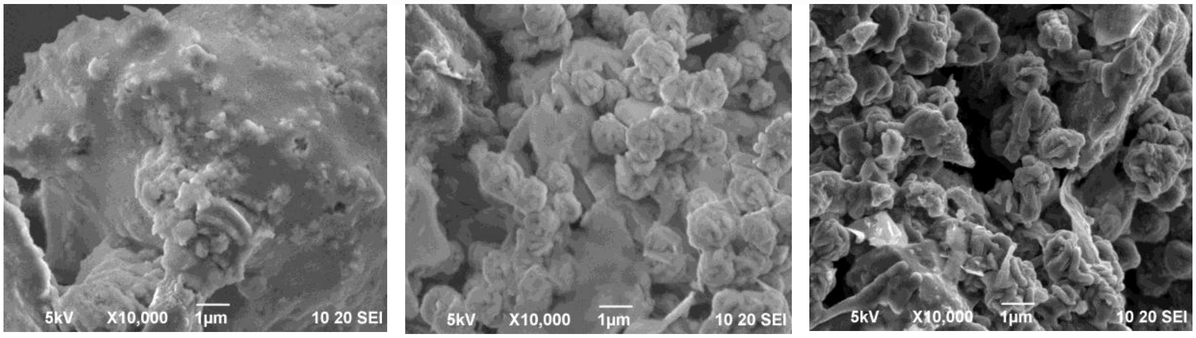

(a) (b) (c)

Figure 1. Activated Carbon-Zeolite composites (a) COM1, (b) COM2, and (c) COM3.

3.2 The Effects of Adsorbent Dosage on Adsorption

The impact of the adsorbent dosage value on the sorbate removal process (from aqueous solutions) is manifested on multiple levels. The effect on the quantity of removal of MB and Pb solution of varying adsorbent dosages was measured by contacting 50 ml of the solution of initial sorbate concentration (of 500 mg/L) at different weighed amounts (0.5, 1, 1.5, 2, and 2.5 g/l) of different adsorbents, using water-bath shakers. This was conducted for a period of five (5) hours and at room temperature (25ºC). At a constant stirring speed of 150 rpm, this gives ample time for the solution to attain equilibrium. Once equilibration is complete, the samples were centrifuged and the supernatant solution’s concentration was measured using the same procedure. The Adsorption percentage was observed to increase as the adsorbent dose rose from 0.5 g - 2 g/l at 500 mg/l lead or dye concentration, based on an equilibrium time of 240 min, as shown in **Fig. 2**, The removal efficiency increases up to the optimum dosage. However, once past this level, there was no observable change in the removal efficiency at greater adsorbent dosages. Nevertheless, it is also apparent that by increasing the adsorbent dose, the amount adsorbed per unit mass decreases, as illustrated in **Fig. 3**. This reduction in adsorption density can be traced to the fact the adsorption sites remain unsaturated, whereas the amount of available adsorption sites grows in line with increases in adsorbent dose, which in turn results in an increase in removal efficiency. This hypothesis seems to be confirmed by the fact that while the adsorption percentage increases sharply for dosage increments between 0.5-2 g/l, the maximal adsorption percentage (of 98%) is achieved at a dosage level of 2 g/l, as clearly shown in Fig. 3. As a result, the 2 g adsorbent dosage was adopted for the rest of the study. However, the lead sorbed-to-adsorbent (mg g^{-1}) ratio decreased with rises in the adsorbent quantity. This decrease in adsorption density as the adsorbent dose increases is to be principally attributed to the non-saturation of the adsorption sites during the adsorption process, as well as to an overlapping between adsorption sites produced by an overcrowding of adsorbent particles, **Garg, et al., 2007**.

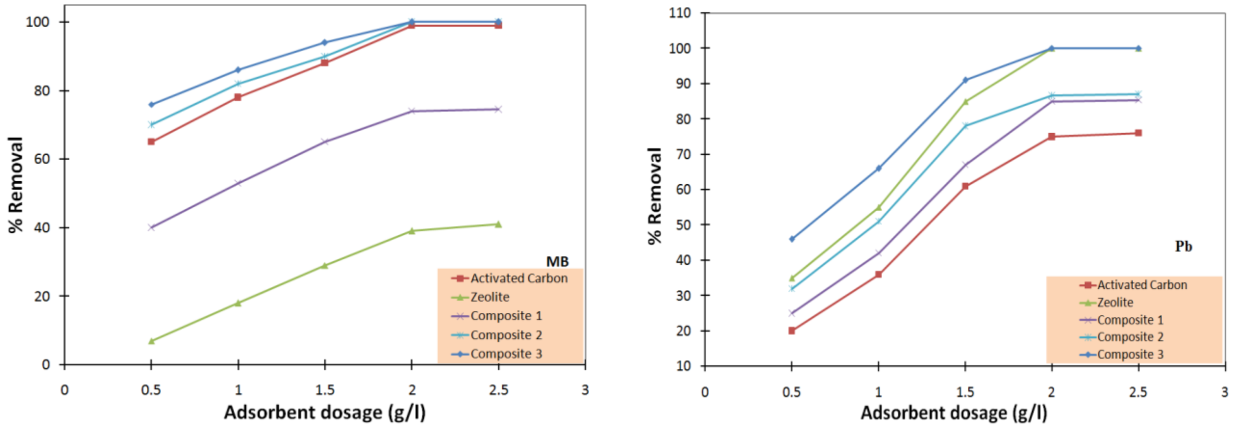

Figure 2. Adsorbent dosage impact on MB/Pb removal for various adsorbents.

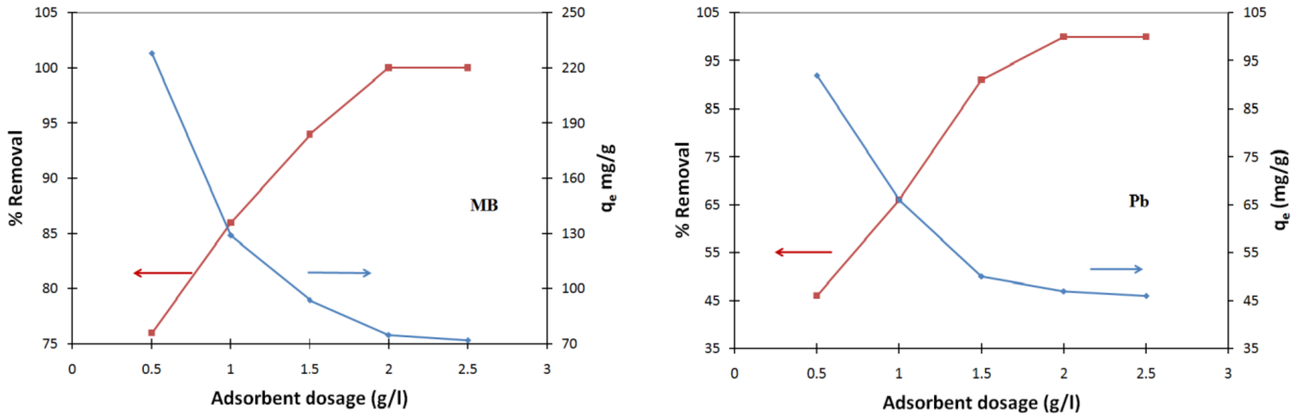

Figure 3. Adsorbent dosage impact on MB/Pb removal and adsorption on Composite 3.

3.3The Effect of Contact Time

The impact of contact time on lead and MB adsorption on Activated Carbon, Zeolite and their composites was investigated so as to examine the rate of their elimination (Fig. 4). It can be easily observed from **Fig. 4** that the percentage of removal of lead metal ions and MB dye rose in line with increases in the duration of contact. Based on an equilibrium time of 240 min, it is obvious that after a contact period of 120 minutes, the observed percentage of removal values for MB, zeolite, COM1, Activated Carbon, COM2 and COM3 were of 33%, 63%, 88%, 94% and 98%, respectively. At the end of the first 60 minutes of contact, the percentage removal can be clearly observed to have risen rapidly in line with increased in the contact duration. The percentage removal subsequently continued to increase gently but slowly until equilibrium was reached. Once equilibrium had been attained, however, any further increases in the duration of contact had a negligible effect on the adsorption capacity of lead and MB.

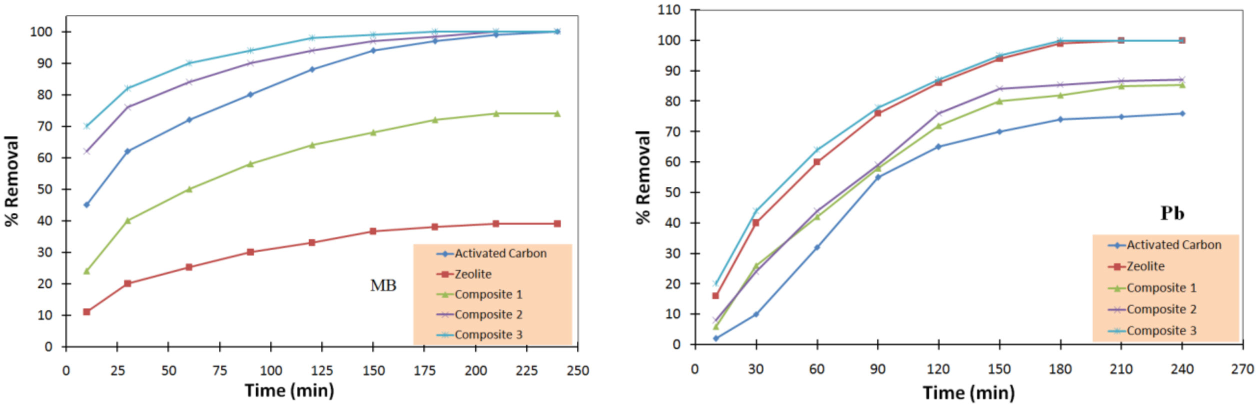

Figure 4. Time of contact impact on MB/Pb removal for various adsorbents.

An examination of these trends suggests that the adsorption performance of lead and MB was greater at the start of the process due to the large number of vacant surface sites available to the adsorption of sorbates. However, as the adsorbed lead ion or MB dye produces a monolayer, the capacity of the adsorbents is exhausted. The uptake rate thus becomes limited by the speed at which the lead ions or MB dye are transferred from the exterior to the interior sites of the adsorbent particles. It must be noted that a particular system will comprise a constant number of active sorption sites. As such, since active sites can adsorb only one ion in a monolayer, the sorbate uptake by the adsorbent surface is likely to be rapid at the start of the process but slow down as the competition intensifies for the decreasingly available energetic sites throughout the sorbate residual in the solution. These results seem to confirm that Activated Carbon, Zeolite and their composites exhibit a very strong ability for adsorption of lead ions and MB in solutions.

3.4 The Effects of Initial Concentration

The initial concentration of the dye or heavy metal ions is an essential parameter in adsorption. This is because a particular amount of adsorbent can only adsorb a correspondingly specific amount of sorbate. The percentage removal of MB or lead was thus examined by varying MB and lead concentrations, from 50 to 500 mg/L, with 2 g/L adsorbent dose of activated carbon, zeolite and their composites. These tests were conducted under the same standard conditions illustrated in **Fig.5**.

Fig. 5 also shows the effects on the adsorption capacity of the adsorbent of the initial concentrations of MB and lead. The adsorption capacity enjoys a steep rise during the initial stages, before levelling off after a specific period of time. This can probably be attributed to the large difference in initial concentrations between the bulk and the surface of the adsorbent, which creates a higher driving force at the beginning of the process. As shown in Figure 5, in the test solution, the actual quantity of sorbate that is adsorbed (per unit mass of the adsorbent) is observed to rise in line with the increase in sorbate concentration. In particular, the adsorbed amount increases from 24 mg/g to 190 mg/g, with an increase in initial concentration from 50 to 500 mg/L for MB. Correspondingly, the adsorbed amount of lead increases form 25 mg/g to 125 mg/g as the initial concentration of lead increases from 50 mg/L to 500 mg/L. In both cases, the adsorption capacity was measured over a period of 200 minutes. The percentage removal, however, was observed to decrease in line with increases in the respective initial concentrations of MB dye or lead. This may be due to the lack of available active sites, which are required for the high initial concentration of sorbate. At low concentrations, the proportion of surface active sites to the total sorbate in the solution is high. In consequence, all MB or Pb ions interact with the adsorbent and are thus quickly eliminated from the solution. According to these results, the initial concentration of MB or lead ions performs a crucial role in determining adsorption capacity. In this regard, it is worth nothing that higher concentrations of metal ions have been used to investigate an adsorbent's maximal adsorption potential, **Mohanty, et al., 2007, and Karthikeyan, et al., 2005**.

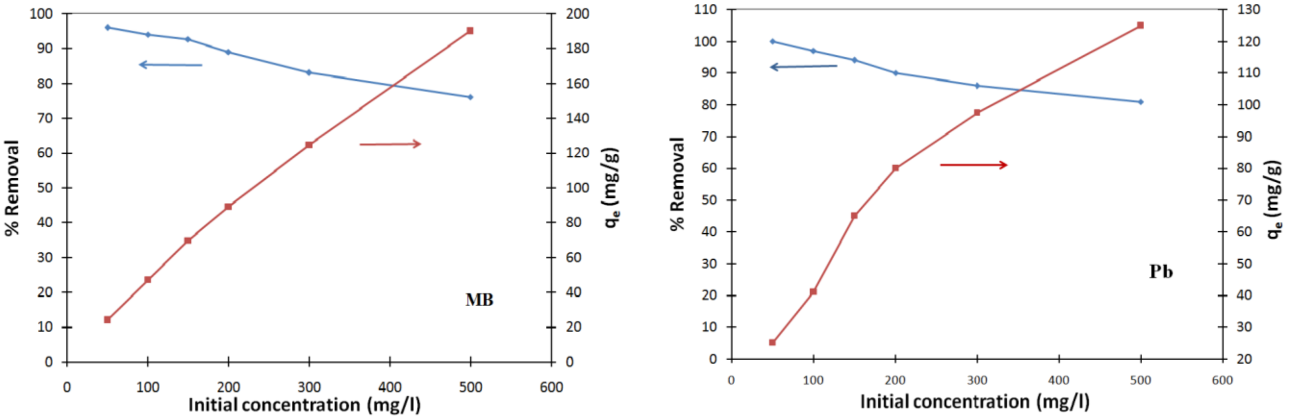

Figure 5. Initial concentration impact on MB/Pb removal and adsorption capacity on Composite 3.

3.5 The Effect of pH

A solution's pH value is clearly one of the most critical parameters in determining the metal and dye's adsorption properties. This partly stems from the crucial effect the pH has not only on the chemical speciation of the sorbate, but also on the ionization of the functional groups onto the adsorbent's surface. Furthermore, the solution's pH value also affects the adsorbent surface's charge properties. In light of this, and in order to properly examine the impact on absorption properties of variations in pH levels a set of experiments were undertaken for a number of different initial pH values, ranging from 2 to 12. These tests were all conducted at a temperature of 25°C. Moreover, once initial pH levels were set by gradually adding HCl or NaOH at the beginning of the experiment, they were not manipulated afterwards. The obtained findings show that MB and Lead adsorption properties were strongly correlated to the solution's pH level. In consequence, batch experiments were conducted to investigate the role played by the concentration of hydrogen ions. It was found that raising the solution's pH results in a reduction in both the competition effect and electrostatic repulsion. As illustrated in **Fig. 6**, for both lead and MB, the amount of adsorption rose in line with increases in pH. Eventually, the adsorption capability is observed to reach a maximal pH value of 6 and 8 respectively. Beyond this maximal point, further increases in pH are observed to bring about no changes in MB's adsorption capability, but produce a reduction in that of lead.

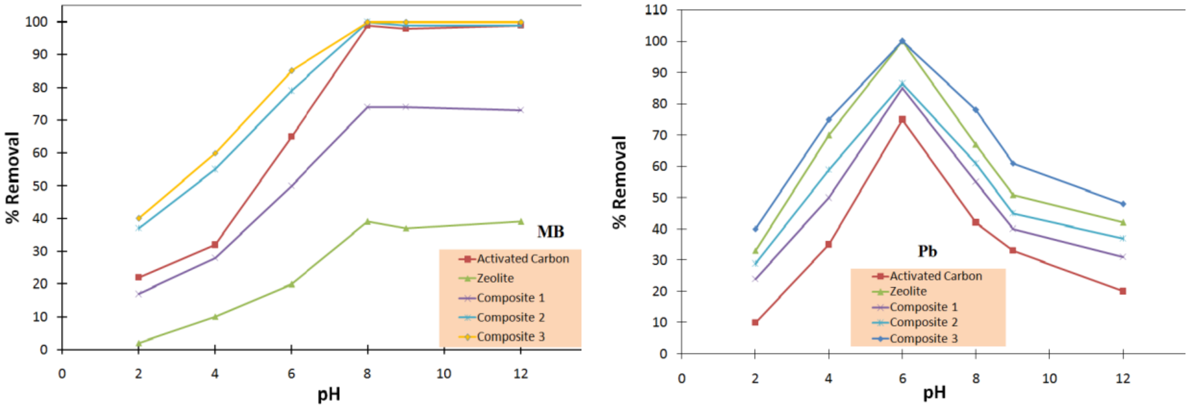

Figure 6. pH effect on MB/Pb removal for various adsorbents.

Similar findings on the impact of pH levels have also been reported for the adsorption of dyes on a number of adsorbents, including banana peel, **Babel, and Kurniawan, 2003**, biological waste slurry, **Yammuna, and Namasivayam, 1993**, and even of Ni^{2+}on orange peel, **Sublet, et al., 2003**. As such, both the surface binding-sites and the aqueous chemistry of the adsorbents are liable to be impacted by the solution's pH levels. For instance, at low pH levels ($pH < 3$), H^+ may compete for the adsorption sites with dye ions. Excessive protonation of the active sites on the adsorbent surface often prevents the formation of links between dye and the active site, which, in turn, inhibits MB adsorption. Furthermore, as the system's pH level decreases, the number of negatively-charged adsorbent sites was also observed to decline accordingly. Conversely, positively-charged surface sites increased in number. Due to electrostatic repulsion, this adversely affects the adsorption of positively-charged dye cations.

Meanwhile, at moderate pH levels ($3< pH <6$), linked H^+ is released from the active sites and, in consequence, a rise in the adsorbed amount of dye ions is generally observed. Findings from the literature indicate that the Pb(II) ions will enter into complexation bonding with functional groups of composite adsorbent. For lead at $pH < 6$, a higher concentration of H+ ions will compete with Pb(II) ions for the adsorbent's surface. This will prevent Pb(II) ions from reaching the sorbet's bonding sites that were produced by the repulsive forces. At $pH > 6$, the Pb(II) ions are observed to undergo sedimentation. This is due to the formation of hydroxide anions, causing a precipitation of lead hydroxide. Since this hydroxylated form of the metal can also compete for the actives sites of the adsorbent with the metal's ions, this adversely affects the adsorption capability, **Panayotova, and Velikov, 2002**. Overall, for a given pH level, the nature of binding events on the composite adsorbent can offer a useful indication of the geometrical coordination's thermodynamic stability.

3.6 Isotherm

The adsorption equilibrium data findings obtained during the tests were analysed using Langmuir and Freundlich isotherms expressions:

$q_e = q_m \, b \, C_e / (1+b \, C_e)$ (2)

$q_e = K \, C_e^{\,n}$ (3)

q_m = maximum sorbate uptake per unit mass of adsorbent (mg/g),

b = Langmuir constant (L/mol).

K_F = Freundlich constant which can be regarded as the indicator of adsorption capacity, and,

1/n = Freundlich constant referring roughly to strength of adsorption or adsorption intensity.

As is commonly the case, linear regression was deployed to establish the best-fitting isotherm. Potential isotherm equations were compared based on the correlation coefficients, so as to determine their applicability. These models are not only well-established and simple to use, they offer a satisfying degree of predictability as well as a physically meaningful interpretation, as can be seen in **Fig.7** and **Tables 1**and **2**.

As shown from **Fig. 7** and **Tables 1** and **2**, it is obvious that the measured isotherm, data for adsorption of led and methylene blue onto activated carbon – zeolite composites are fitted well both Langmuir and Freundlich models. However, it is clear that by comparing the correlation coefficients (R^2) for both models, the Freundlich isotherm are slightly higher than that for Langmuir isotherm. As the Freundlich isotherm proposed a multilayer adsorption which is suitable for both types of surfaces, homogenous and heterogeneous. This suggests the heterogeneity of the adsorbent surface which is made up of small heterogeneous sites but they are homogenous in themselves. The mechanism of surface exchange leads to increase the adsorption sites formed by activation process, **Wanees, et al, 2012**.

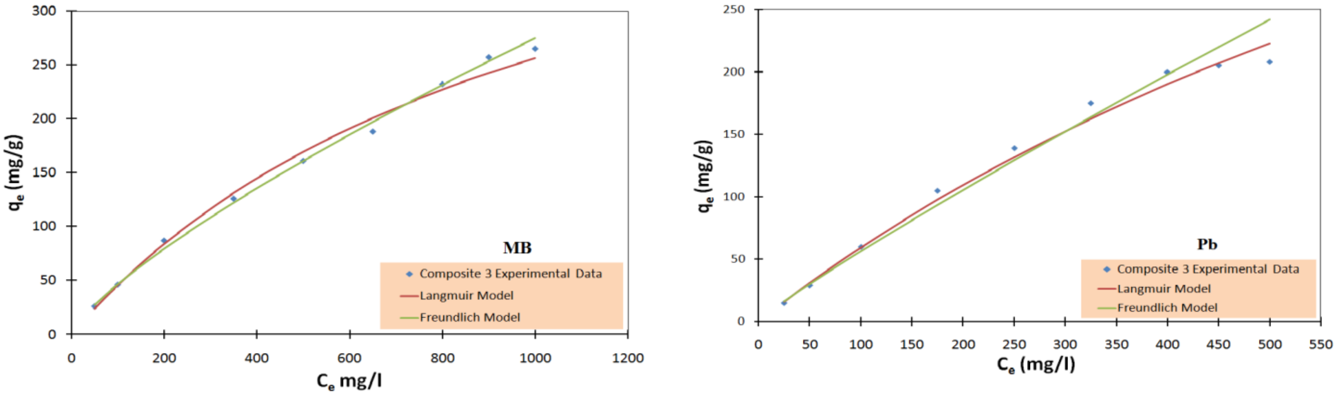

Figure 7. Langmuir vs Freundlich models for experimental MB/Pb adsorption results on Composite 3.

Table 1. Adsorption isotherm parameters, correlation coefficient and predicted adsorption capacity for Langmuir isotherm for adsorption of MB.

Adsorbent	**Activated Carbon**		**Zeolite**		**Composite 1**		**Composite 2**		**Composite 3**	
Langmuir Model Parameters	q_m = 370.370 **b** = 0.001756 R^2 = 0.9975		q_m = 131.579 **b** = 0.001125 R^2 = 0.9970		q_m = 454.546 **b** = 0.000651 R^2 = 0.742		q_m = 526.316 **b** = 0.000652 R^2 = 0.8503		q_m = 588.235 **b** = 0.000949 R^2 = 0.9499	
No.	q_e**(exp.)**	q_e**(pred.)**	q_e**(exp.)**	q_e**(pred.)**	q_e**(exp.)**	q_e**(pred.)**	q_e**(exp.)**	q_e**(pred.)**	q_e**(exp.)**	q_e**(pred.)**
1	30.01	29.896	7.02	7.007	14.98	14.338	18.9	18.560	25.44	23.854
2	55.12	55.327	13.11	13.305	32.05	27.798	39.79	35.985	46.03	45.640
3	95.36	96.273	24.99	24.166	50.64	52.393	69.04	67.820	86.89	83.997
4	140.41	140.999	37.05	37.170	86.89	84.392	105.63	109.239	126.57	131.280
5	172.09	173.164	47.16	47.366	101.26	111.674	133.58	144.552	161.81	169.431
6	200.03	197.423	55.11	55.574	115.53	135.21	157.72	175.015	188.73	200.862
7	219.98	216.367	62.08	62.324	153.42	155.723	191.19	201.564	231.94	227.205
8	227.14	226.848	67.97	66.195	187.93	167.994	229.66	217.446	256.77	242.519
9	230.72	235.993	69.33	69.657	189.78	179.297	246.95	232.074	264.91	256.341

Table 2. Adsorption isotherm parameters, correlation coefficient and predicted adsorption capacity for Freundlich isotherm for adsorption of MB.

Adsorbent	**Activated Carbon**		**Zeolite**		**Composite 1**		**Composite 2**		**Composite 3**	
Freundlich Model Parameters	**K**= 2.343 **n** = 0.6813 R^2 = 0.9867		**K**= 0.3925 **n** = 0.7616 R^2 = 0.9914		**K**= 0.6683 **n** = 0.816 R^2 = 0.9904		**K**= 0.8513 **n** = 0.8172 R^2 = 0.9946		**K**= 1.3298 **n** = 0.7717 R^2 = 0.9971	
No.	q_e**(exp.)**	q_e**(pred.)**	q_e**(exp.)**	q_e**(pred.)**	q_e**(exp.)**	q_e**(pred.)**	q_e**(exp.)**	q_e**(pred.)**	q_e**(exp.)**	q_e**(pred.)**
1	30.01	33.667	7.02	7.723	14.98	16.268	18.9	20.821	25.44	27.219
2	55.12	53.988	13.11	13.093	32.05	28.639	39.79	36.686	46.03	46.472

3	95.36	86.575	24.99	22.198	50.64	50.421	69.04	64.639	86.89	79.339
4	140.41	126.758	37.05	33.994	86.89	79.603	105.63	102.119	126.57	122.192
5	172.09	161.625	47.16	44.604	101.26	106.495	133.58	136.677	161.81	160.909
6	200.03	193.258	55.11	54.469	115.53	131.919	157.72	169.36	188.73	197.021
7	219.98	222.626	62.08	63.802	153.42	156.276	191.19	200.679	231.94	231.260
8	227.14	241.227	67.97	69.789	187.93	172.042	229.66	220.956	256.77	253.265
9	230.72	259.179	69.33	75.621	189.78	187.487	246.95	240.823	264.91	274.718

3.7 Adsorption Kinetics

Adsorption kinetics models allow for evaluating the solute's uptake rate. The latter is a crucial parameter in determining the residence time of the adsorbate uptake at the solid–solution interface, as well as the diffusion process. The adsorption's rate and mechanisms are determined by a plethora of factors. These include not only the nature and various properties – both physical and chemical - of the adsorbent, but also the solution's pH levels and the medium's ambient temperature.

Thus, with regards to designing and optimising effluent treatment processes, such kinetic models are highly valuable. A number of kinetic models have been deployed over the years to examine and test adsorption kinetics and, ultimately, to adequately characterise the adsorptive interactions between Pb, MB and the adsorbent.

In the context of the present work, the models adopted in the examination and analysis of the data include:

Pseudo-first order equations.
Pseudo-second order equations.
Second order kinetic equations.

The linear forms for each of these three equations, respectively, are as follows:

$$ln\left(1-\frac{q_e}{q_t}\right)=-K_1t \qquad (4)$$

$$\frac{t}{q_t}=\frac{1}{K_2q_e^2}+\frac{t}{q_e} \qquad (5)$$

$$\frac{1}{q_e-q_t}=\frac{1}{q_e}+Kt \qquad (6)$$

Where, q_e and q_t represent the amount of dye adsorbed per adsorbent unit mass (mg/g) at equilibrium and at time t (min), respectively. K1, K2 and K are the constants of equilibrium for pseudo first order, pseudo second order and second order kinetics equations

Using the slopes and intercepts of the linear plots of the respective kinetic equations, the relevant kinetic parameters are obtained. Based on the obtained linear regression coefficient (R^2) values, the analysis of the experimental data shows that the pseudo-second order equation (Eq. 5) offers the best description. In particular, the analysis shows that Equation 5 exhibits the most linear fit, providing correlation coefficients of R^2= 0.996 and 0.999 for Pb and MB, respectively. Moreover, the values of both experimental q_t and calculated q_t were observed to be close in convention. This seems to further suggest the applicability of pseudo-second order kinetic model (**Fig. 8).** For the adsorption of MB and Pb on activated carbon – zeolite composite, it is clear from the experimental data, (as shown in Figure 8), that the initial adsorption rate is rapid followed by slower rate. At the beginning, there are a lot of vacant adsorption sites which are ready to interact with the sorbate, so the adsorption is higher. Also the driving force for adsorption is higher initially due to the large concentration difference between the bulk solution and solid-liquid interface. Diffusion of sorbent into the adsorbent became slower after the initial period leading to slow adsorption rate.

The transfer of Pb and MB from the solution phase into the adsorbent's surface pores should also be taken into account, as it is highly indicative of the rate controlling step in batch experiments (during a fast mixing setting), **Rafie, and Mei, 2014**.

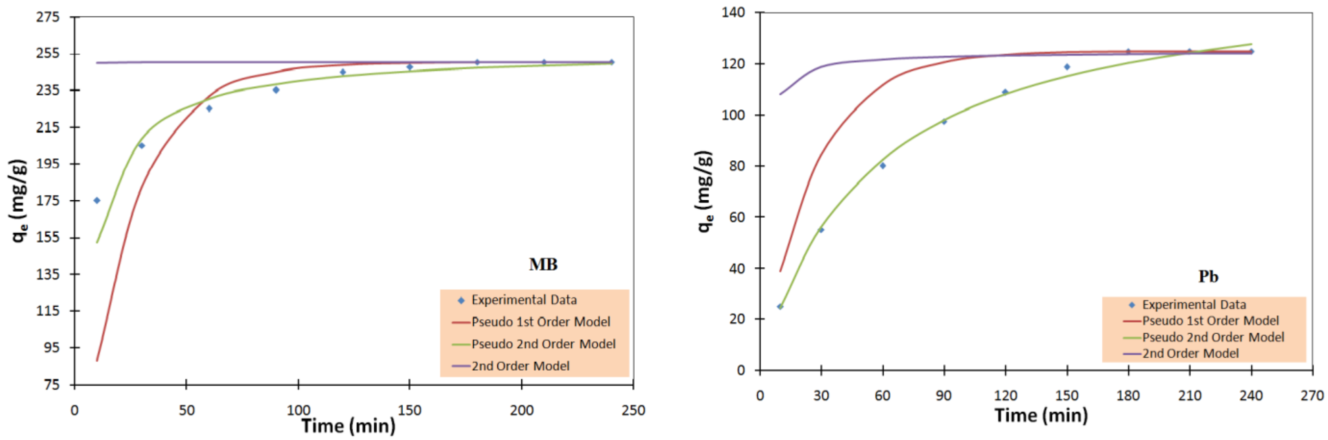

Figure 8. Different MB-Pb adsorption kinetic models on Composite 3

4. CONCLUSION

The present work examines the adsorption of MB and Pb from aqueous solutions onto Activated Carbon (AC), Zeolite, and three different AC-Zeolite composites. Analyses of the findings point to a number of conclusions. Composites were well prepared and have shown great potential for use in applications involving the removal of MB and Pb from aqueous solutions. The composite adsorbents that have been produced exhibit a high surface area. The present investigation also shows that, of all the materials under examination, Composite 3 is the most effective adsorbent. Adsorption capacity of the various adsorbents was shown to be highly dependent on a number of parameters, including the initial MB and Pb concentrations, the adsorbent dosage, the duration of contact, and the solution's pH. The results also show that the optimum pH, corresponding to the maximum adsorption rate, was found to be 8 and 6, for MB and Pb respectively. The efficiency of MB- and Pb-removal was shown to rise in line with increases in the adsorbent dosage and contact duration. However, it was also shown to decrease as the initial concentration of the adsorbate solution increased. The adsorption data were found to be well-fitted by the

Freundlich and Langmuir isotherm models. Of all the kinetic models tested, the adsorption kinetics was best described, for both sorbates, by the pseudo-second order equation.

REFERENCES

- Akl, M., Mostafa, M. M., and Mohammed, S. B., 2016, *Enhanced Removal of Some Cationic Dyes from Environmental Samples Using Sulphuric Acid Modified Pistachio Shells Derived Activated Carbon*, J Chromatogr Sep. Tech., Vol. 7, No. 4, PP. 1-10.
- Babel, S., Kurniawan, T. A., 2003, *Low Cost Adsorbent for Heavy Metals Uptake from Contaminated Water: A Review*, J. Hazard. Mater., Vol. 97, PP. 219–243.
- Bulut, Y., and Aydin, H., 2006, *A Kinetic and Thermodynamics Study of Methylene Blue Adsorption on Wheat Shells*, Desalination, Vol. 194, No. 1-3, PP. 259-267.
- Chakrabarti, S., and Dutta, B. K., 2005, *Adsorption of Methylene Blue onto Jute Fiber Carbon: Kinetics and Equilibrium Studies*, Journal of Colloid and Interface Science, Vol. 284, No. 1, PP. 78-82.
- Chen, W., 2001, *Treatment of Wastewater from Electroplating by 13X Molecular Sieve*, Cailiao Baohu, Vol. 34, No. 2, PP. 45–46.
- Dabrowski, A., Podkoscielny, P., Hubicki, Z., and Barczak, M., 2005, *Adsorption of Phenolic Compounds by Activated Carbon: A Critical Review*, Chemosphere, Vol. 58, PP. 1049-1070.
- Doğan, M., Alkan, M., Turkyilmaz, A., and Ozdemir, Y., 2004, *Kinetics and Mechanism of Removal of Methylene Blue by Adsorption onto Perlite*, Journal of Hazardous Materials, Vol. 109, No. 1-3, PP. 141-148.
- Ebrahimian, P. A., Hashemian, S.F., and Yousefi, A., 2015, *Surfactant-Modified Wheat Straw: Preparation, Characterization and its Application for Methylene Blue Adsorption from Aqueous Solution*, J Chem Eng Process Technol, Vol. 6, No.3, PP. 1-9.
- Eisazadeh A., Hossein E., and Khairul A. K., 2013, *Removal of Pb(II) Using Polyaniline Composites and Iron Oxide Coated Natural Sand and Clay from Aqueous Solution, Synthetic Metals*, Vol. 171, PP. 56-61.
- Foo, K.Y., and Hameed, B.H., 2011, *The Environmental Applications of Activated Carbon/Zeolite Composite Materials*, Adv. Colloid Interface Sci., Vol. 162, 22–28.
- Garg, V. K., Gupta, R., Yadav, A. B., and Kumar, R., 2003, *Dye Removal from Aqueous Solution by Adsorption on Treated Sawdust*m Bioresource Technology, Vol., 89, PP.121–124.
- Garg, U. K., Kaur, M. P., Garg, V. K., and Sud, D., 2007, *Removal of Hexavalent Chromium from Aqueous Solution by Agricultural Waste Biomass*, Hazard. Mater., Vol. 140, PP. 60-68.
- Ghosh, D., and Bhattacharyya,K. G., 2002, *Adsorption of Methylene Blue on Kaolinite*, Applied Clay Science, Vol. 20, No. 6, PP. 295-300.
- Giraldo, L., and Piraján, J. C., 2008, Pb_2^+ *Adsorption from Aqueous Soluotions on Activated Carbons Obtained from Lignocellulosic Residues*, Brazilian Journal of Chemical Engineering, Vol. 25, No. 01, pp. 143–151.
- Gong, L., Sun, W., and Kong, L., 2013,*Adsorption of Methylene Blue by NaOH-modified Dead Leaves of Plane Trees*, Computational Water, Energy, and Environmental Engineering, Vol. 2, PP. 13-19.

- Gurses, A., Karaca, S., Doğar C., Bayrak R., Açıkyıldız M., and Yalc, M., 2004, *Determination of Adsorptive Properties of Clay/Water System: Methylene Blue Sorption*, Journal of Colloid and Interface Science, Vol. 269, No. 2, PP. 310-314.
- Haochun, S., Weisong, L., Lei, Z., and Chunjian, X., 2014, *Methylene Blue Adsorption from Aqueous Solution by Magnetic Cellulose/Graphene Oxide Composite: Equilibrium, Kinetics, and Thermodynamics*, Ind. Eng. Chem. Res., Vol. 53, No. 3, PP. 1108–1118.
- Hashemian, S., Ardakani, M., and Salehifarm H., 2013, *Kinetics and Thermodynamics of Adsorption Methylene Blue onto Tea Waste/*$CuFe_2O_4$ *Composite*, American Journal of Analytical Chemistry, Vol. 4, PP. 1-7
- Imamura, K., Ikeda, E., Nagayasu, T., Sakiyama, T., and Nakinishi K., 2002, *Adsorption Behavior of Methylene Blue and Its Congeners on a Stainless Steel Surface*, Journal of Colloid and Interface Science, Vol. 245, No. 1, PP. 50-57.
- Inglezakis, V. J., Loizidou, M. D., and Grigoropoulou, H. P.m 2003, *Ion Exchange of* Pb_2C*,* Cu_2C*, and* Cr_3C *on Natural Clinoptilolite: Selectivity Determination and Influence of Acidity on Metal Uptake,* J. Colloid Int. Sci, Vol. 261, PP. 49–54.
- Jeminat, O. A., Jose, H. S., Zahangir M. A., Aminul H. M., Chan C. M., 2016, *Adsorption of methylene blue from aqueous solution using untreated and treated (Metroxylon spp.) waste adsorbent: equilibrium and kinetics studies*, Int J Ind Chem, Vol. 7, PP. 333–345.
- Kamble, S.P., Mangrulkar, P.A., Bansiwal, A.K., and Ragalu, S.S., 2008. *Adsorption of Phenol and Ochlorophenol on Surface Altered Fly Ash Based Molecular Sives*, Chemical Engineering Journal, Vol. 138, PP. 73-83.
- Karthikeyan, T., Rajgopal, S., and Miranda, L. R., 2005, *Chromium Adsorption from Aqueous Solution by Hevea Brasilinesis Sawdust Activated Carbon*, J. Hazard. Mater., Vol. 124, PP. 192-199.
- Krowiak, A., Szafran, R. G., and Modelski, S., 2011, *Bio-Sorption of Heavy Metals from Solutions onto Peanut Shell as a Low-Cost Biosorbent*, Desalination, Vol. 265, No. 1-3, PP. 126-134.
- Kumaar, S., Varadarajan, P. R., Porkodi, K. and Subbhuraam, C. V., 2005, *On the Adsorption and Diffusion of Methylene Blue in Glass Fibers*, Journal of Colloid and Interface Science, Vol. 286, No. 2, PP. 807-811.
- Kumar, K. V., Ramamurthi, V., and Sivanesan, S., 2005, *Modelling the Mechanism Involved during the Sorption of Methylene Blue onto Fly Ash*, Journal of Colloid and Interface Science, Vol. 284, No. 1, pp. 14-21.
- Legrouri, K., Khouya, E., Hannache, H., El Hartti, M., Ezzine, M., and Naslain, R., 2017, *Activated Carbon from Molasses Efficiency for Cr(VI), Pb(II) and Cu(II) Adsorption: A Mechanistic Study*, Chemistry International, Vol. 3, No. 3, PP. 301-310.
- Ming, C, Yun, C., and Guowang D., 2010, *Adsorption Kinetics and Thermodynamics of Methylene Blue onto p-tert-Butyl-calix[4,6,8]arene-Bonded Silica Gel*, J. Chem. Eng. Data, Vol. 55, No. 11, PP. 5109–5116.
- Mohanty, K., Jha, M., Meikap, B. C., and Biwas, M. N., 2006, *Biosorption of Chromium(VI) from Aqueous Solution by Eichhornia Crassipis,* Chem. Eng. J., Vol. 117, PP. 71-77.

- Mostafa A.A., Youssef, H. F., Sorour, M.H., Tewfik, S. R., and Shalaan, H. F., 2011, *Utilization of Egyptian kaolin for Zeolite-A Preparation and Performance Evaluation*, 2nd International Conference on Environmental Science and Technology IPCBEE, Vol. 6, PP. 43-48.
- Nasuha, V., Hameed, B. H., and Mohd Din, A.T., 2010, *Rejected Tea as a Potential Low-Cost Adsorbent for the Removal of Methylene Blue*, Journal of Hazardous Materials, Vol. 175, No. 1-3, PP. 126-132.
- Nnaji, C. C., Chinwe, J. E., and Emmanuel, I. U., 2017, *Physicochemical Conditions for Adsorption of Lead from Water by Rice Husk Ash*, BioResources, Vol. 12, No. 1, PP. 779-818.
- Olin, T. J., and Bricka, R. M., 1998, *Zeolite: a Single Use Sorbent for the Treatment of Metals-Contaminated Water and Waste Streams*, Min. Eng. (Littleton, Colorado), Vol. 50, No. 11, PP. 61–66.
- Ouki, S. K., and Kavannagh, M., 1999, *Treatment of Metals Contaminated Waste Waters by Use of Natural Zeolites*, Water Sci. Technol., Vol. 39, No. 10, PP. 115–122.
- Panayotova, M., and Velikov, B., 2002, *Kinetics of Heavy Metal Ions Removal by Use of Natural Zeolite*, J. Environ. Sci. Health, Vol. 37, No. 2, PP.139–147.
- Petruzzelli, D., Pagano, M., Tiravanti, G., and Passino, R., 1999, *Lead Removal and Recovery from Battery Waste Waters by Natural Zeolite Clinoptilolite*, Solvent Extr. Ion Exch., Vol. 17, No. 3, PP. 677–694.
- Rafatullah, M., Sulaiman, O., Hashim, R. and Ahmad, A., 2010, *Adsorption of Methylene Blue on Low-Cost Adsorbents: A Review*, Journal of Hazardous Materials, Vol. 177, p. 70–80.
- Rafie R. M., and Chong, M. F., 2014, *Treatment and Decolorization of Biologically Treated Palm Oil Mill Effluent (POME) Using Banana Peel as Novel Biosorbent*, Journal of Environmental Management, Vol. 132, PP. 237-249.
- Rhoda, H., Rhoda, G., Gumus, H., 2016, *Kinetic Studies of Methylene Blue Adsorption on to Activated Carbon Prepared from Plantain Pod (Musa paradisiac),* British Journal of Applied Science & Technology, Vol. 15, No. 3, PP. 1-14.
- Ruchi, S., Richa, S., Sangeeta T., and Sandeep K. T., 2016, *Surface Engineered Zeolite: An Active Interface for Rapid Adsorption and Degradation of Toxic Contaminants in Water*, ACS Appl. Mater. Interfaces, Vol. 8, No. 19, PP. 12520–12527.
- Shams, K., and Mirmohammadi, S. J., 2007, *Preparation of 5A Zeolite Monolith Granular Extrudates using Kaolin: Investigation of the Effect of Binder on Sieving/Adsorption Properties Using a Mixture of Linear and Branched Paraffin Hydrocarbons*, Microporous and Mesoporous Materials, Vol. 106, PP. 268–277.
- Shisuo F., Wang, Y., Wang, Z., Tang, J., Jun T., and Xuede L., 2017, *Removal of Methylene Blue from Aqueous Solution by Sewage Sludge-Derived Biochar: Adsorption Kinetics, Equilibrium, Thermodynamics and Mechanism,* Journal of Environmental Chemical EngineeringVol. 5, No. 1, PP. 601–611.
- Shukla, Y., Zhang, H., Dubey, P., Margrave, S., and. Shuklam, S., 2002, *The Role of Sawdust in the Removal of Un- wanted Materials from Water*, Journal of Hazardous Materials, Vol. 95, No. 1-2, PP. 137-152.

- Standeker, S., Novak, Z., and Knez, Ž. 2007. *Adsorption of Toxic Orangic Compounds from Water with Hydrophobic Silica Aerogels*, Journal of Colloid, Vol. 18, PP. 128-136.
- Sublet, R., Simonnot, M. Q., Boireau, A., Sardin, M., 2003, *Selection of an Adsorbent for Lead Removal from Drinking Water by a Point of Use Treatment Device*, Water Res., Vol. 37, PP. 4904–4912.
- Tamez U., Akhtarul Islam, S. Mahmud, J. L., and. Rukanuzzaman, *Adsorptive Removal of Methylene Blue by Tea Waste*," Journal of Hazardous Materials, Vol. 164, No. 1, PP. 53-60.
- Tepamat, T., Mongkolkachit, C., and Wasanapiarnpong, T.,2014, *Syenthesis of Zeolite NaA and Activated Carbon Composite From Rice Husk*, Suranaree J. Sci. Technol., Vol. 21, No. 2, PP. 119-123.
- Tholiso N., Jabulani R. G., Vhahangwele M., and Arjun M., 2017, *An Update on Synthetic Dyes Adsorption onto Clay Based Minerals: A State-of-Art Review*, Journal of Environmental Management , Vol. 191, No.15, PP 35–57.
- Torrellas, S. Á., Ovejero, G., Lovera, R. G., Rodríguez, A., García, J., 2016, *Synthesis of a Mesoporous Carbon from Peach Stones for Adsorption of Basic Dyes from Wastewater: Kinetics, Modeling, and Thermodynamic Studies*, Clean Technologies and Environmental Policy, Vol. 18, No. 4, PP. 1085–1096.
- Vadivelan, V., and Kumar, K. V., 2005, *Equilibrium, Kinetics, Mechanism, and Process Design for the Sorption of Methylene Blue onto Rice Husk*, Journal of Colloid and In- terface Science, Vol. 286, No. 1, PP. 90-100.
- Wanees, S. A, Ahmed, A. M., Adam, M. S. and Mohamed, M. A., 2012, *Adsorption Studies on the Removal of Hexavalent Chromium-Contaminated Wastewater using Activated Carbon and Bentonite*, Vol. 02, No. 03, PP. 95-105.
- Yammuna, R. T., and Namasivayam, C., 1993, *Color Removal from Aqueous Solution by Biogas Residual Slurry*, Toxicol. Environ. Che., Vol. 38, PP. 131–143.